

Quantitative Test of Thermal Field Theory for Bose-Einstein Condensates

S. A. Morgan,¹ M. Rusch,² D. A. W. Hutchinson,³ and K. Burnett²

¹*Department of Physics and Astronomy, University College London, Gower Street, London WC1E 6BT, United Kingdom*

²*Clarendon Laboratory, Department of Physics, University of Oxford, Parks Road, Oxford OX1 3PU, United Kingdom*

³*Department of Physics, University of Otago, P.O. Box 56, Dunedin, New Zealand*

(Received 22 May 2003; published 18 December 2003)

We present numerical results from a second-order quantum field theory of Bose-Einstein condensates applied to the 1997 JILA experiment [D. S. Jin *et al.*, Phys. Rev. Lett. **78**, 764 (1997)]. Good agreement is found for the energies and decay rates for both the lowest-energy $m = 2$ and $m = 0$ modes. The anomalous behavior of the $m = 0$ mode is due to experimental perturbation of the noncondensate. The theory is gapless and includes the coupled dynamics of the condensate and thermal cloud, the anomalous pair average, and all relevant finite size effects.

DOI: 10.1103/PhysRevLett.91.250403

PACS numbers: 03.75.Kk, 05.30.Jp, 67.40.Db

One of the most intriguing consequences of the experimental realization of Bose-Einstein condensation (BEC) was the prospect of quantitative tests of finite-temperature quantum field theory (QFT). The pioneering measurements of condensate excitations at JILA provide the most stringent tests to date of such theories [1,2]. Accurate calculations are difficult, however, because of the need to include the dynamic coupling of condensed and uncondensed atoms simultaneously with effects of strong interactions and finite size. In this Letter, we describe the first direct comparison of a second-order QFT calculation with the JILA measurements. The results show that accurate tests of QFT are possible if it is properly adapted to the finite, driven systems under consideration. Our method is general and can be applied directly to a wide variety of recent experiments on BECs [3–6].

Measurements of excitations at low temperature are in good agreement with predictions based on the Gross-Pitaevskii equation (GPE) and Bogoliubov quasiparticles [1,7,8]. However, the finite-temperature JILA results [2] have proved much harder to explain. In this experiment the energies of the lowest modes with axial angular momentum quantum numbers $m = 2$ and $m = 0$ were measured as a function of reduced temperature $t = T/T_c^0$, where T is the absolute temperature and T_c^0 is the BEC critical temperature for an ideal gas. The $m = 2$ mode was observed to shift downwards with t , while the $m = 0$ mode underwent a sharp increase in energy at $t \sim 0.6$ towards the result expected in the noninteracting limit.

The temperature dependence of the excitations has been studied theoretically using the Popov approximation to the Hartree-Fock-Bogoliubov formalism, where the anomalous (pair) average of two condensate atoms is neglected. This gives good agreement with experiment for low temperatures but cannot explain the results for $t > 0.6$ [9]. Good agreement for all t for the $m = 2$ mode was obtained using an extension of this approach, which includes the anomalous average [10], and also within the dielectric formalism [11]. However, both approaches were

unable to explain the upward shift of the $m = 0$ mode, and an analytical calculation also predicted downward shifts for both modes [12]. The importance of the relative phase of condensate and noncondensate fluctuations was emphasized in [13], where the JILA results for $m = 0$ were qualitatively explained by a shift from out-of-phase to in-phase oscillations at high temperature. Jackson and Zaremba (JZ) [14] obtained good quantitative agreement for both modes using a GPE for the condensate coupled to a noncondensate modeled by a Boltzmann equation. However, this approach neglects the phonon character of low-energy states as well as the anomalous average and Beliaev processes. The anomalous average can be significant [10,15] and Beliaev processes have been directly observed in a number of recent experiments [6,16–18]. It is therefore important to develop a theory which systematically includes these effects.

In this Letter, we describe such a theory and demonstrate its validity by obtaining good agreement with the JILA experimental results [2]. In particular, we are able to explain straightforwardly the anomalous behavior of the $m = 0$ mode. The theoretical approach was developed by one of us (S. M.) as an extension of an earlier second-order perturbative calculation [15,19]. The formalism adapts the linear response treatment of Giorgini [12] and closely models the experimental procedure where excitations are created by small modulations of the trap frequencies. The result is a gapless extension of the Bogoliubov theory which includes the dynamic coupling between the condensate and noncondensate, all relevant Beliaev and Landau processes, and the anomalous average. It is also consistent with the generalized Kohn theorem for the dipole modes [20]. The theory is valid in the collisionless limit of well-defined quasiparticles, which requires $(k_B T/n_0 U_0)(n_0 a_s^3)^{1/2} \ll 1$, where n_0 is the condensate density, a_s is the s -wave scattering length, k_B is Boltzmann's constant, and $U_0 = 4\pi\hbar^2 a_s/m$, where m is the atomic mass [12,15]. For the JILA experiment [2] this parameter does not exceed 0.03 at the trap center for the highest temperature we consider.

The theory starts from the generalized GPE for the condensate wave function $\Phi(\mathbf{r}, t)$

$$i\hbar \frac{\partial \Phi}{\partial t} = [\hat{H}_{\text{sp}} + P(\mathbf{r}, t) - \lambda(t) + N_0(t)U_0|\Phi|^2]\Phi + 2U_0\tilde{n}(\mathbf{r}, t)\Phi + U_0\tilde{m}(\mathbf{r}, t)\Phi^* - f(\mathbf{r}, t). \quad (1)$$

Here $\hat{H}_{\text{sp}} = -\hbar^2\nabla^2/2m + V_{\text{trap}}(\mathbf{r})$ is the static single-particle Hamiltonian, $P(\mathbf{r}, t)$ is the time-dependent external perturbation, and $\lambda(t)$ is a scalar. The noncondensate density $\tilde{n}(\mathbf{r}, t)$, anomalous average $\tilde{m}(\mathbf{r}, t)$, and $f(\mathbf{r}, t)$ are constructed from time-dependent quasiparticle wave functions $u_i(\mathbf{r}, t)$ and $v_i(\mathbf{r}, t)$ by

$$\tilde{n}(\mathbf{r}, t) = \sum_i |u_i(\mathbf{r}, t)|^2 N_i + |v_i(\mathbf{r}, t)|^2 (N_i + 1), \quad (2)$$

$$\tilde{m}(\mathbf{r}, t) = \sum_i u_i(\mathbf{r}, t)v_i^*(\mathbf{r}, t)(2N_i + 1), \quad (3)$$

$$f(\mathbf{r}, t) = \frac{1}{N_0} \sum_i c_i^* N_i u_i(\mathbf{r}, t) + c_i (N_i + 1) v_i^*(\mathbf{r}, t), \quad (4)$$

$$c_i(t) = N_0 U_0 \int d\mathbf{r} |\Phi|^2 [\Phi^* u_i(\mathbf{r}, t) + \Phi v_i(\mathbf{r}, t)]. \quad (5)$$

The quasiparticle wave functions evolve according to

$$i\hbar \frac{\partial}{\partial t} \begin{pmatrix} u_i \\ v_i \end{pmatrix} = \begin{pmatrix} \hat{L} & \hat{M} \\ -\hat{M}^* & -\hat{L}^* \end{pmatrix} \begin{pmatrix} u_i \\ v_i \end{pmatrix}, \quad (6)$$

$$\hat{L}(\mathbf{r}, t) = \hat{H}_{\text{sp}} + P(\mathbf{r}, t) + N_0 U_0 [|\Phi|^2 + \hat{Q}|\Phi|^2\hat{Q}], \quad (7)$$

$$\hat{M}(\mathbf{r}, t) = N_0 U_0 \hat{Q}\Phi^2\hat{Q}^*, \quad (8)$$

where the projector $\hat{Q} = \delta(\mathbf{r} - \mathbf{r}') - \Phi(\mathbf{r}, t) \int d\mathbf{r}' \Phi^*(\mathbf{r}', t)$ ensures orthogonality of $\Phi(\mathbf{r}, t)$ and $\{u_i(\mathbf{r}, t), v_i^*(\mathbf{r}, t)\}$.

The quasiparticle populations $\{N_i\}$ are independent of time and given by the Bose-Einstein distribution $N_i = 1/(e^{\epsilon_i/k_B T} - 1)$, where ϵ_i is the Bogoliubov energy (see below). Most quantities in the theory depend on temperature via these populations. The condensate population $N_0(t)$ is defined in terms of the fixed total number of particles N by $N_0(t) = N - \int d\mathbf{r} \tilde{n}(\mathbf{r}, t)$. The zero-temperature part of the anomalous average $\tilde{m}(\mathbf{r}, t)$ is ultraviolet (UV) divergent, but it can be renormalized straightforwardly [12,15,19]. Equations (1)–(8) are obtained using the number-conserving approach of Gardiner and Castin and Dum, modified for finite-temperature calculations [19,21–23]. The terms $f(\mathbf{r}, t)$ and \hat{Q} are a feature of this approach and do not appear in symmetry-breaking theories. We find that they can give a significant contribution to the energy shifts.

In the static case, Eq. (1) has a time-independent solution $\Phi(\mathbf{r}, t) = \Phi(\mathbf{r})$ which satisfies

$$[\hat{H}_{\text{sp}} - \lambda + N_0 U_0 |\Phi(\mathbf{r})|^2 + 2U_0 \tilde{n}(\mathbf{r})]\Phi(\mathbf{r}) + U_0 \tilde{m}(\mathbf{r})\Phi^*(\mathbf{r}) - f(\mathbf{r}) = 0, \quad (9)$$

where λ is the condensate eigenvalue. Setting $\tilde{n}(\mathbf{r})$, $\tilde{m}(\mathbf{r})$, and $f(\mathbf{r})$ to zero gives the usual GPE with wave function $\Phi_0(\mathbf{r})$ and energy λ_0 . We solve Eq. (9) by linearizing the change in energy and shape relative to this solution. Writing $\Phi \rightarrow \Phi_0(\mathbf{r})$ in Eq. (6), we obtain static quasiparticle wave functions $u_i(\mathbf{r}, t) = u_i(\mathbf{r})e^{-i\epsilon_i t/\hbar}$, $v_i(\mathbf{r}, t) = v_i(\mathbf{r})e^{-i\epsilon_i t/\hbar}$, and the Bogoliubov energies $\{\epsilon_i\}$. These solutions are used to construct $\tilde{n}(\mathbf{r})$, $\tilde{m}(\mathbf{r})$, and $f(\mathbf{r})$ and provide a convenient basis for the subsequent calculation.

Applying the perturbation $P(\mathbf{r}, t)$ gives all quantities a small time-dependent oscillation around their static values, $\Phi(\mathbf{r}, t) = \Phi(\mathbf{r}) + \delta\Phi(\mathbf{r}, t)$, $\tilde{n}(\mathbf{r}, t) = \tilde{n}(\mathbf{r}) + \delta\tilde{n}(\mathbf{r}, t)$, etc. Substituting this into Eq. (1) and linearizing, we obtain the equation of motion for the condensate fluctuation $\delta\Phi(\mathbf{r}, t)$. This equation can be solved by combining it with its complex conjugate, Fourier transforming and expanding the fluctuation in the static quasiparticle basis

$$\begin{pmatrix} \delta\Phi(\mathbf{r}, \omega) \\ \delta\Phi^*(\mathbf{r}, -\omega) \end{pmatrix} = \sum_i b_i(\omega) \begin{pmatrix} u_i(\mathbf{r}) \\ v_i(\mathbf{r}) \end{pmatrix}. \quad (10)$$

The expansion coefficients $b_i(\omega)$ are directly related to the condensate density fluctuations $\delta n_0 = \delta(N_0|\Phi|^2)$, which are measured experimentally.

Dynamics of the noncondensate can occur via two distinct mechanisms; either it is driven directly by the perturbation or indirectly via the condensate. If we neglect the first possibility and assume that only the single mode p is excited, then $b_p(\omega)$ is given by

$$b_p(\omega) = P_{p0}(\omega) \mathcal{G}_p(\omega + i\gamma). \quad (11)$$

Here $P_{p0}(\omega)$ is the matrix element for the generation of the excitation from the condensate and $i\gamma$ is a small imaginary part in the frequency (discussed below). The resolvent $\mathcal{G}_p(\omega)$ is defined in terms of a self-energy $\Sigma_p(\omega)$ by

$$\mathcal{G}_p(\omega) = \frac{1}{\hbar\omega - \epsilon_p - \Sigma_p(\omega)}, \quad (12)$$

$$\Sigma_p(\omega) = \Delta E_p^{(S)} + \Delta E_p^{(D)}(\omega). \quad (13)$$

$\Sigma_p(\omega)$ contains two types of energy shifts, static (S) and dynamic (D), corresponding to the different roles of the thermal cloud. The static term $\Delta E_p^{(S)}$ comes from interactions between a condensate fluctuation and the static noncondensate mean fields. The dynamic term $\Delta E_p^{(D)}(\omega)$ describes the driving of the noncondensate by the condensate and its subsequent backaction, which leads to damping and energy shifts of condensate excitations. The inclusion of this contribution gives a gapless excitation spectrum [12,15].

However, the noncondensate can also be excited directly by the external perturbation and can then generate condensate fluctuations. This process therefore changes the effective excitation matrix element P_{p0} and can be included by replacing $\mathcal{G}_p(\omega + i\gamma)$ in Eq. (11) with the modified resolvent $\mathcal{R}_p(\omega + i\gamma)$, defined by

$$\mathcal{R}_p(\omega) = \left[1 + \frac{\Delta P_{p0}^{(S)}(\omega) + \Delta P_{p0}^{(D)}(\omega)}{P_{p0}(\omega)} \right] \mathcal{G}_p(\omega). \quad (14)$$

The important extra term here is $\Delta P_{p0}^{(D)}(\omega)$, which describes the generation of noncondensate fluctuations by the perturbation and their subsequent coupling to the condensate. $\Delta P_{p0}^{(S)}(\omega)$ describes the effect of changes in the static condensate shape [$\Phi_0(\mathbf{r}) \rightarrow \Phi(\mathbf{r})$].

The detailed definition of $\Delta E_p^{(D)}$ and $\Delta P_{p0}^{(D)}$ is lengthy and is given elsewhere [19,24]. We note here that they are both calculated as a sum over many Landau and Beliaev processes, which are resonant whenever an energy matching criterion is satisfied. The parameter γ in Eq. (11) is required to keep $\Delta E_p^{(D)}$ and $\Delta P_{p0}^{(D)}$ finite at the resulting poles. Its inclusion can be formally justified from the finite experimental resolution and its value is of order the inverse of the observation time. Our numerical results are essentially independent of this parameter for physically relevant values.

If Σ_p and $\Delta P_{p0}^{(D)}$ are roughly independent of frequency, the energy shift can simply be calculated from the poles of \mathcal{G} , i.e., the solutions to $E_p = \hbar\omega_p = \text{Re}[\epsilon_p + \Sigma_p(\omega_p)]$, while the decay rate is given by $\Gamma_p = -\text{Im}[\Sigma_p(\omega_p)]/\hbar$. This situation arises in homogeneous condensates where an excitation couples to a continuum of decay channels and the resolvents are Lorentzians. For a finite system, however, $\Sigma_p(\omega)$ depends on frequency, and neither $\mathcal{G}_p(\omega)$ nor $\mathcal{R}_p(\omega)$ are perfect Lorentzians. In this case, we extract energies and decay rates by fitting $b_p(\omega)$ to a complex Lorentzian plus a constant. The frequency dependence of $P_{p0}(\omega)$ is included as a (known) weight function in the fit and γ is subtracted from the resulting decay rate. This corresponds to the experimental procedure of fitting a decaying sinusoid to the condensate density fluctuations in the time domain.

We present numerical results for the parameters of the JILA experiment [2]. We consider a condensate of $N_0 = 6000$ ^{87}Rb atoms in an axisymmetric harmonic trap with radial and axial trap frequencies of $\omega_r/2\pi = 129$ Hz, $\omega_z/2\pi = 365$ Hz. The scattering length is $110a_0$, where a_0 is the Bohr radius. We fix N_0 for all the temperatures considered (consistent with the experiment for $t < 0.9$) and include zero-temperature effects using the appropriate UV renormalization [19]. The external perturbation is $P(\mathbf{r}, t) \propto r^2 \cos(m_p \phi - \omega_d t)$, where r and ϕ are the radial and azimuthal angle coordinates and $\omega_d \approx \epsilon_p/\hbar$ is the central drive frequency. The parameter γ is $0.036\hbar\omega_r$ [2].

For a fixed N_0 we first solve the static GPE of Eq. (9) with $\tilde{n} = \tilde{m} = f = 0$ to obtain $\Phi_0(\mathbf{r})$. We then calculate and store the quasiparticle basis functions $u_i(\mathbf{r})$ and $v_i(\mathbf{r})$ and unperturbed energies ϵ_i from the static limit of Eq. (6) for all states up to an energy cutoff $E_{\text{cut}} \sim 130\hbar\omega_r$. Using these we can construct all static and dynamic terms, defined by sums and integrals over various functions of the quasiparticles. The numerical calculation is difficult because of the need to describe low-energy states accu-

rately while also converging significant single-particle effects. We therefore use a Gaussian quadrature scheme together with a large value of E_{cut} and a semiclassical approximation at high energy [12]. The final results are converged to within $5 \times 10^{-3}\hbar\omega_r$. Further details are given in [25].

Results for the $m = 2$ and $m = 0$ modes are compared to experiment in Fig. 1. As can be seen, the theory predicts a significant downwards shift for the $m = 2$ mode. The agreement with experiment is reasonable if we consider the temperature error in the measurements (of order 5%–10%), which is not shown. The downward curvature of the results is due to the scaling of the temperature axis from absolute to reduced temperature. For $k_B T \gg \lambda_0$ the shift is linear in T , as expected theoretically [12].

If we neglect direct driving of the noncondensate, then similar behavior is seen for the $m = 0$ mode, as in previous calculations [10–12]. Including this effect gives very different results, however, and the theory correctly reproduces the sharp upward shift in the excitation energy around $t = 0.6$. This is because an r^2 perturbation couples strongly to single-particle modes with frequency differences of $2\omega_r$, so the noncondensate response is peaked in this region. The effect on the condensate is shown in Fig. 2, where the resolvents \mathcal{G} and \mathcal{R} are plotted as a function of frequency and temperature. The appearance of a growing peak at $\omega = 2\omega_r$ in \mathcal{R} is due to direct driving of the noncondensate and is absent in \mathcal{G} . In this case the perturbation excites mainly the thermal cloud, which then drives the condensate, rather than the reverse. This coincides with a change in the relative phase of the oscillations, from generally out of phase at low t to in

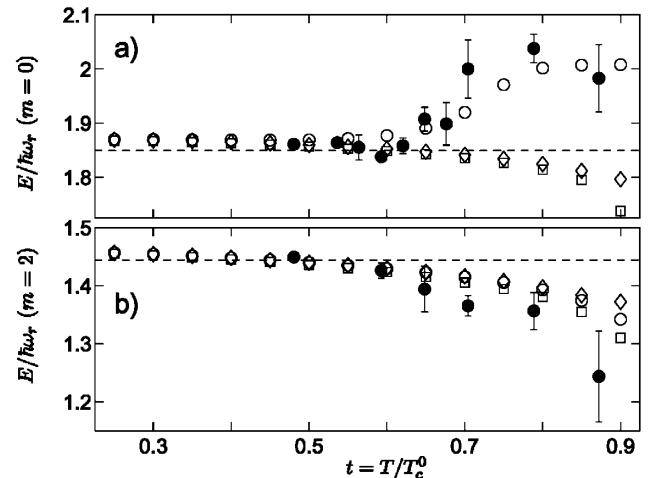


FIG. 1. *Ab initio* theoretical excitation energies E (open symbols) compared with experiment (solid circles) for (a) $m_p = 0$ and (b) $m_p = 2$. Diamonds neglect direct thermal driving (\mathcal{G}_p), open circles include it (\mathcal{R}_p), and squares give E_p . The dashed line is the Bogoliubov energy ϵ_p . Differences between diamonds and squares are due to non-Lorentzian structure in \mathcal{G}_p . There are no free parameters in the theoretical results.

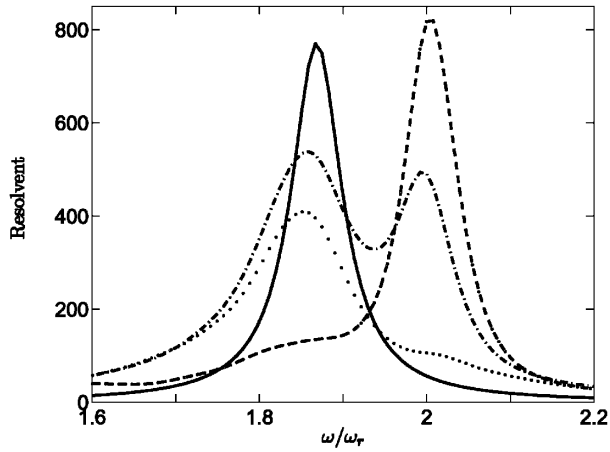


FIG. 2. $|\mathcal{R}_p(\omega) \times \hbar\omega_r|^2$ for $m_p = 0$ as a function of frequency for $t = 0$ (solid line), $t = 0.65$ (dot-dashed line, $\times 4$) and $t = 0.9$ (dashed line, $\times 4$). For comparison, $|\mathcal{G}_p(\omega) \times \hbar\omega_r|^2$ is shown at $t = 0.65$ (dotted line, $\times 4$).

phase at high t , consistent with the argument in [13]. The out-of-phase branch should be observable using a perturbation localized around the condensate.

Figure 3 shows the results for the damping rates. Overall, the agreement with experiment is good and consistent with other calculations [11,14,26]. The overestimate of the damping at low t was also seen in [14] and may be due to experimental difficulties in measuring low temperatures. For $m = 0$, the damping is underestimated at high t if direct driving of the thermal cloud is included. This is partly due to uncertainties in extracting widths from non-Lorentzian spectra at high temperature [25].

Our results are consistent with the recent calculations of JZ [14] indicating that the anomalous average and Beliaev processes play a relatively minor role in the JILA experiment. Nonetheless, the low temperature shifts we obtain arise purely from these processes (cf. Fig. 1) and they are essential to describe other recent experiments [6,16,17]. A detailed discussion of the relation between the two calculations will be given elsewhere [25].

In conclusion, we have developed a gapless theory of BEC excitations at finite temperature and demonstrated its validity by comparison with the JILA experiment [2]. Good agreement is found for the energies and decay rates of the lowest modes with $m = 2$ and $m = 0$. The anomalous behavior of the $m = 0$ mode is the result of direct excitation of the noncondensate by the external perturbation. These results show that a consistent perturbative approach is appropriate for the finite-temperature dynamics of BECs, contrary to statements in the literature [11,14]. Our method can therefore be used as a general tool to study the finite-temperature response of Bose condensates beyond the Bogoliubov approximation.

S. M. thanks the Royal Society and Trinity College, Oxford for support and M. J. Davis and S. A. Gardiner for many useful discussions. K. B. thanks the Royal Society

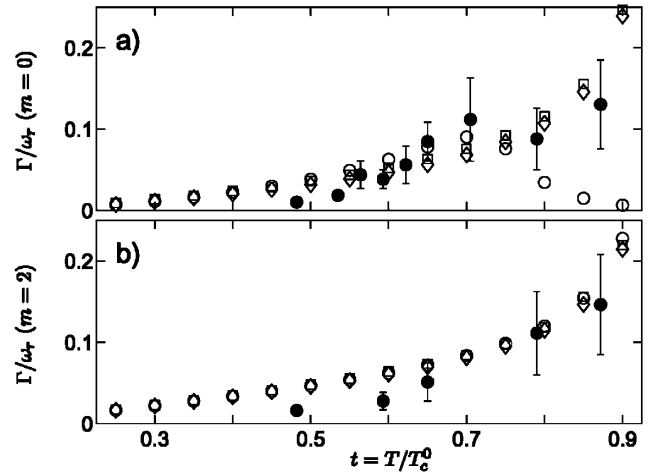


FIG. 3. Theoretical decay rates (Γ) compared with experiment for (a) $m_p = 0$ and (b) $m_p = 2$. Symbols are as in Fig. 1.

and the Wolfson Foundation. D. A. W. H. thanks the Marsden Fund of the Royal Society of New Zealand.

-
- [1] D. S. Jin *et al.*, Phys. Rev. Lett. **77**, 420 (1996).
 - [2] D. S. Jin *et al.*, Phys. Rev. Lett. **78**, 764 (1997).
 - [3] D. M. Stamper-Kurn *et al.*, Phys. Rev. Lett. **81**, 500 (1998).
 - [4] O. Maragò *et al.*, Phys. Rev. Lett. **86**, 3938 (2001).
 - [5] F. Chevy *et al.*, Phys. Rev. Lett. **88**, 250402 (2002).
 - [6] V. Bretin *et al.*, Phys. Rev. Lett. **90**, 100403 (2003).
 - [7] S. Stringari, Phys. Rev. Lett. **77**, 2360 (1996).
 - [8] M. Edwards *et al.*, Phys. Rev. Lett. **77**, 1671 (1996).
 - [9] R. J. Dodd *et al.*, Phys. Rev. A **57**, R32 (1998).
 - [10] D. A. W. Hutchinson, R. J. Dodd, and K. Burnett, Phys. Rev. Lett. **81**, 2198 (1998).
 - [11] J. Reidl *et al.*, Phys. Rev. A **61**, 043606 (2000).
 - [12] S. Giorgini, Phys. Rev. A **61**, 063615 (2000).
 - [13] M. J. Bijlsma and H. T. C. Stoof, Phys. Rev. A **60**, 3973 (1999); U. Al Khawaja and H. T. C. Stoof, *ibid.* **62**, 053602 (2000).
 - [14] B. Jackson and E. Zaremba, Phys. Rev. Lett. **88**, 180402 (2002).
 - [15] S. A. Morgan, J. Phys. B **33**, 3847 (2000).
 - [16] E. Hodby *et al.*, Phys. Rev. Lett. **86**, 2196 (2001).
 - [17] N. Katz *et al.*, Phys. Rev. Lett. **89**, 220401 (2002).
 - [18] T. Mizushima, M. Ichioka, and K. Machida, Phys. Rev. Lett. **90**, 180401 (2003).
 - [19] S. A. Morgan, cond-mat/0307246 [Phys. Rev. A (to be published)].
 - [20] J. F. Dobson, Phys. Rev. Lett. **73**, 2244 (1994).
 - [21] C. W. Gardiner, Phys. Rev. A **56**, 1414 (1997).
 - [22] Y. Castin and R. Dum, Phys. Rev. A **57**, 3008 (1998).
 - [23] S. A. Morgan and S. A. Gardiner (unpublished).
 - [24] The structure of these terms is similar to Eq. (80) of [15], but with different matrix elements.
 - [25] S. A. Morgan (unpublished).
 - [26] P. O. Fedichev, G. V. Shlyapnikov, and J. T. M. Walraven, Phys. Rev. Lett. **80**, 2269 (1998).